Sánchez, R., Newman, D. E., & Mier, J. A. (2018). Modeling transport across the running-sandpile cellular automaton by means of fractional transport equations. *In Physical Review E, 97*(5), 052123-052133

DOI: 10.1103/physreve.97.052123

Modelling transport across the running sandpile cellular automaton by means of fractional transport equations

R. Sánchez[1*], D. E. Newman[2] and J. A. Mier[3]
[1] *Departamento de Física, Universidad Carlos III de Madrid, 28911 Leganés, Madrid, Spain*
[2] *Department of Physics, University of Alaska, Fairbanks, AK 99775-5920, USA*
[3] *Departamento de Física Aplicada, Universidad de Cantabria, 39005 Santander, Spain*
(Dated: April 10, 2018)

Fractional transport equations are used to build an effective model for transport across the running sandpile cellular automaton [T. Hwa and M. Kardar, *Phys. Rev.* A **45**, 7002 (1992).]. It is shown that both temporal and spatial fractional derivatives must be considered to properly reproduce the sandpile transport features, that are governed by self-organized criticality, at least over sufficiently long/large scales. In contrast to previous applications of fractional transport equations to other systems, the specifics of sand motion require in this case that the spatial fractional derivatives used for the running sandpile must be of the completely asymmetrical Riesz-Feller type. Appropriate values for the fractional exponents that define these derivatives in the case of the running sandpile are obtained numerically.

I. INTRODUCTION

Sandpile cellular automata became the posterchild for self-organized criticality (SOC) from the very early days[1], and many variants have been constructed to provide simplified frameworks in which the complex dynamics of many different systems could be studied, from earthquakes to forest fires, from solar flares to accretion disks[2–8] [Although, curiously enough, it has been proven[9,10] that these automata do not provide a good description of natural sandpile dynamics!]. All of these automaton variants contain, in one way or another, the main ingredients needed for SOC dynamics to appear: an open, driven system with a local instability threshold and a large separation of scales between local drive and instability relaxation. The resulting dynamic steady state, once the external drive and sandpile losses are balanced on average, is known as the SOC state[1]. It exhibits properties typical of critical points such as scale-invariance, long-term memory and divergent correlations. Transport through the system is inherently bursty and of non-diffusive nature, being dominated by avalanches.

In the field of magnetically confined fusion (MCF) toroidal plasmas, a variant of the sandpile automaton known as the running sandpile[11–14] has been used extensively to try to understand turbulent transport characteristics in tokamaks and stellarators[15]. A main feature of the running sandpile, that somewhat moves it away from other sandpile automata often discussed in the literature, is that the separation between the timescales of drive and relaxation is finite and, sometimes, not very large. This comes about because, in contrast to the standard sandpile automaton, the drive is not stopped once an avalanche starts and reactivated after all avalanching activity dies away. Instead, the sandpile keeps on being driven as avalanches progress in time. This choice of rules makes both analytical progress and numerical characterization of avalanches more challenging (avalanches do overlap, for instance) but, at the same time, introduces a time scale in the problem that is essential for many practical applications and, in particular, in the context of MCF plasmas[15–17].

Among the many needs of the MCF tokamak program, an important one is the development of effective mean-field transport models with reliable predictive capabilities regarding the confinement of the plasma density and energy in these toroidal traps[18]. Several authors have suggested that, at least in those plasma regimes in which SOC-like dynamics appear to dominate radial transport, these effective models would require the use of fractional transport equations[15,19–23]. In this article, we describe in detail how one such effective transport model could be built for the running sandpile cellular automaton, given its role as a simple, but still meaningful paradigm for the transport dynamics taking place in MCF plasmas while in a SOC-like regime. The results reported here, albeit meaningful in their own right within the context of the study of sandpile automata, might also teach some useful lessons regarding the construction of effective models in MCF plasmas, as well as for any other natural systems with similar directed transport dynamics.

The article is thus organized as follows: in Sec. II the running sandpile automaton is briefly introduced. Then, an effective transport equation is built for the running sandpile in Sec. III starting from a continuous-time random walk (CTRW) model that incorporates the most salient features of transport in the sandpile. The resulting effective transport equation contains both fractional derivatives in space and time. The most relevant free parameters that define the fractional transport model, namely its fractional exponents, are then quantified numerically in Sec. IV, with the help of tracers (i.e., marked

*Corresponding author: raul.sanchez@uc3m.es

grains of sand). We will then proceed to discuss the meaning of these results in Sec. V and draw some final conclusions in Sec. VI.

II. THE RUNNING SANDPILE MODEL

The sandpile celluar automaton that we will consider in this paper is the one-dimensional, driven and directed running sandpile[11,12] (see Fig. 1). The sandpile domain consists of L cells or sites, numbered from $n = 1$ to $n = L$. To each cell n, a variable h_n is assigned that represents the amount of sand stored (or its height) in the cell.

The running sandpile state is evolved in time in the following way. First, by randomly dropping N_b grains of sand on every cell at each iteration with a probability P_0. What happens next depends on the value of the local slope at each of the sandpile cell. A critical slope exists, $-Z_c$ ($Z_c > 0$) that, when locally overcome (i.e., when the local gradient $Z_n = h_{n+1} - h_n$ exceeds $-Z_c$), causes the removal of N_f grains of sand to the adjacent position. All cells are checked for instability once per iteration. After this is done, a new iteration starts, and new sand is randomly dropped over the sandpile cells. The rules of the running sandpile are completed by imposing a closed boundary condition at $n = 1$, so that no sand flux enters that cell from the left, and an open boundary condition at $n = L$, so that all sand grains reaching the bottom edge of the sandpile (in chunks of N_f, since they must be transported by avalanches; rain is not added to the last cell!) are removed from the system.

The SOC character of the sandpile transport dynamics is rooted in the existence of this critical slope. In addition, it is also important that the relaxation process has some inertia. That is, that $N_f > N_b$, to avoid the average slope staying at the critical value $-Z_c$ all the time. Also, it must happen that $N_f > P_0 N_b L$ in order to avoid the sandpile becoming overdriven. The reason for this condition is that, since the sandpile receives $P_0 N_b L$ grains of sand per iteration (on average), steady-state requires this value to be less than what can be extracted at the sandpile edge per iteration, given by N_f.

The running sandpile will always reach a steady state under a continuous, fixed-average external drive. The average slope of the sandpile, at steady state, is roughly given by $\bar{Z} \simeq -(Z_c - N_f/2)$ due to the aforementioned inertia of the relaxation (see Fig. 2; an explicit estimation of the average slope in the running sandpile is given, for instance, in Ref. 24; an alternative estimation is provided in Ref. 25). Transport across the sandpile domain will be driven by avalanches, that exhibit an approximately self-similar distribution of linear sizes and durations over an extended range of scales (or *mesorange*) that is limited only by finite size effects[12]. Avalanche initiation points are roughly uniformly distributed throughout the pile, except at the very edge, where the open boundary condition imposes a larger mean slope. The probability of an avalanche stopping increases with the cell index, n, due to the fact[25] that the sand that needs to be transported down the slope must increase to balance the integrated drive over all cells $n' < n$. Furthermore, the time series of the sandpile activity, defined as the number of unstable cells at each time, exhibits long-term persistence over scales much longer than the maximum avalanche duration[12,26]. In particular, persistence in the running sandpile has been extensively studied using, among other methods, its power spectrum (that scales as f^{-a}, $0 < a < 1$ over the SOC mesorange) or determining

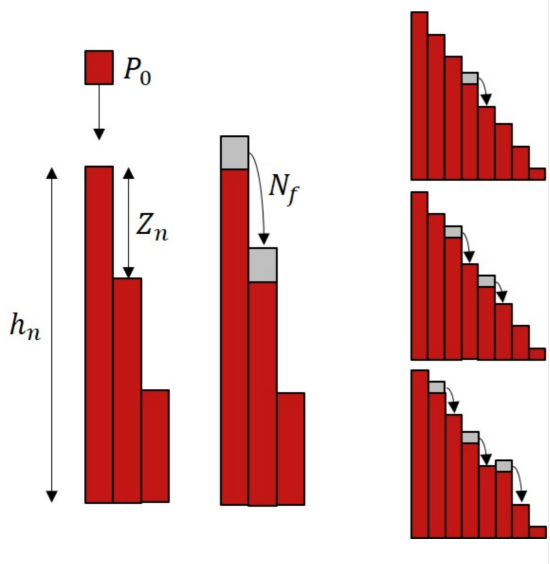

FIG. 1: (Color online) (left) Sketch of the one-dimensional sandpile in real space explaining the corresponding automaton rules. (right) Sketch of an avalanche taking place.

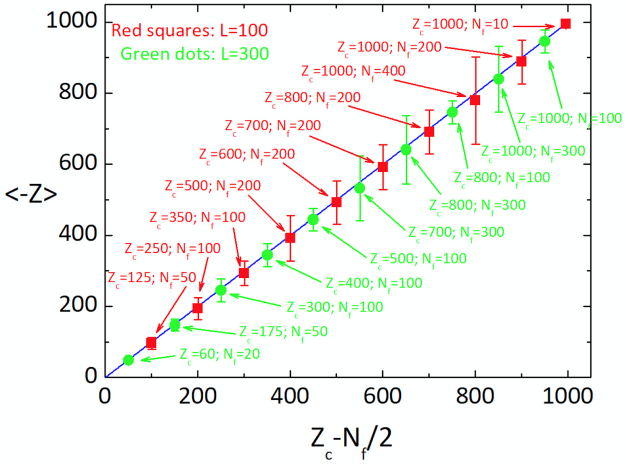

FIG. 2: (Color online) Plot of the average sandpile slope, $-\langle Z \rangle$, vs the estimate $-(Z_c - N_f/2)$ for two sandpiles with lengths $L = 100$ (in red/dark grey squares) and $L = 300$ (in green/light grey circles) and various values of N_F and Z_c. The error bars represent the standard deviation, that naturally scales with N_F.

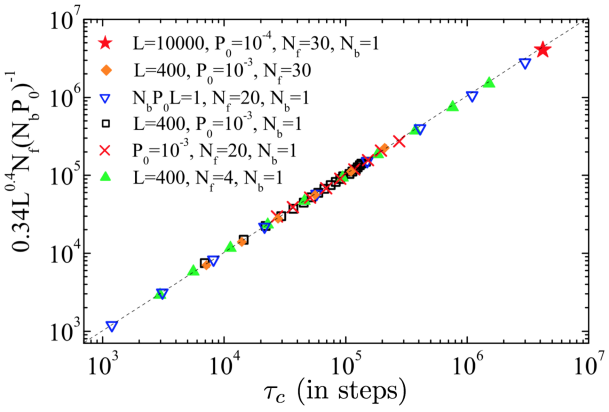

FIG. 3: (Color online) Global scaling of the mean value of the transit time (τ_c) with sandpile parameters L, N_f, N_b and P_0.

its Hurst exponent (that satisfies $H > 0.5$ over the SOC mesorange timescales).

In order to characterize the particle confinement in the sandpile from a global perspective, it is useful to measure the average time taken for a marked grain of sand to move across the whole sandpile and reach the edge. We will later describe in detail how these marked grains are advanced (see Sec. IV). For now, it suffices to say that their average confinement time τ_c has been estimated using a large number of marked grains and then fit to a product of powers of the main sandpile parameters. Namely, the sandpile length L, the number of grains locally moved when unstable N_f, the number of grains dropped on every cell at each iteration N_b and the rain probability P_0 [The critical threshold Z_c does not affect the confinement time. It has been set to $Z_c = 200$ in all simulations.]. The resulting global scaling for τ_c is (see also, Fig. 3):

$$\tau_c = 0.34 L^{0.4} N_f \left(N_b P_0\right)^{-1}. \tag{1}$$

Clearly, the most remarkably feature of this global scaling law, that reveals its non-diffusive (i.e., avalanche) dynamics, is the value of the L-exponent.

III. MEAN FIELD TRANSPORT MODEL FOR THE RUNNING SANDPILE AUTOMATON IN TERMS OF FRACTIONAL DERIVATIVES

In this section, we will construct an effective mean field transport model for the running sandpile just described. The starting point is the well-known continuous-time random walk (CTRW) formalism[27], that we have adapted to the reality of transport in the running sandpile automaton. The effective transport model results from considering the long-time, large-distance asymptotic behaviour of this CTRW, as it has traditionally been done for many other problems[28]. In the one-dimensional CTRW, a number of walkers N are considered. Each walker stays at its initial position, x_0, for a *waiting time* Δt. Then, it carries out a *jump* of size Δx, that takes the walker to its new position, $x_0 + \Delta x$. This process is carried out many times by each walker. The CTRW is defined, naturally, by prescribing the pdf of both jump sizes, $p(\Delta x)$, and waiting-times, $\psi(\Delta t)$. In a purely diffusive system, the transport process is expected to have finite characteristic scales, both in time and space (in a gas, for instance, these scales could be the mean free path and the inverse collision frequency, respectively). In a SOC system, however, the self-similar, critical nature of the SOC state prevents these characteristic scales from existing. The choices for p and ψ must then naturally reflect these features, as will be discussed soon. These waiting-times will endow the CTRW with an interesting property, that is sometimes referred to as a semi-Markovian character. Namely, it refers to the fact that in spite of the waiting-times being identically distributed and independent random variables, their accumulation introduces a memory in the absence of a finite first moment, and thus non-Markovian properties[29].

Before getting any deeper into that discussion, it is however convenient to solve the CTRW. By that, we mean to calculate its propagator, $G(x,t|x_0,t_0)$, as a function of the choices made for $p(\Delta x)$ and $\psi(\Delta t)$. The propagator simply gives the probability of finding one walker at position x and time t, assuming it was at position x_0 at a previous time t_0. Once known, the general solution of the CTRW can be written, for arbitrary initial (i.e., $t = 0$) walker density, $n_0(x)$ and external source of walkers, $S(x,t)$ as:

$$\begin{aligned} n(x,t) &= \int_{-\infty}^{\infty} dx' G(x,t|x',0) n_0(x') + \\ &+ \int_0^t dt' \int_{-\infty}^{\infty} dx' G(x,t|x',t') S(x',t'). \end{aligned} \tag{2}$$

By defining an augmented source as $S^{\rm aug}(x,t) = S(x,t) + n_0(x)\delta(t)$, we can recast this equation as:

$$n(x,t) = \int_0^t dt' \int_{-\infty}^{\infty} dx' G(x,t|x',t') S^{\rm aug}(x',t'). \tag{3}$$

Since the CTRW is invariant under translations in both space and time (or, in other words, since the pdfs p and ψ do not explicitly depend on the position x of the walker or the current time t), it then follows that the propagator only depends on the relative distance and the elapsed time, which turns Eq. 3 into:

$$n(x,t) = \int_0^t dt' \int_{-\infty}^{\infty} dx' G(x-x',t-t') S^{\rm aug}(x',t'). \tag{4}$$

This double convolution combines well with the fact that the propagator of the CTRW can straightforwardly be found in Fourier-Laplace space, as shown in Ref. 27. It is given by:

$$\bar{G}(k,s) = \frac{(1-\tilde{\psi}(s))/s}{1-\tilde{\psi}(s)\hat{p}(k)}. \tag{5}$$

Here, s and k respectively stand for the Laplace and Fourier variables related to Δt and Δx. The Laplace transform is represented by a tilde on top of the function being transformed, the Fourier transform by a hat, whilst the double Laplace-Fourier transform by a bar.

A mean field transport model can now be built by first proposing suitable choices for $p(\Delta x)$ and $\psi(\Delta t)$, and then keeping just the long-time, large-distance asymptotic behaviour of the resulting propagator. In Fourier-Laplace space, this means taking the asymptotic behaviour for $k \to 0$ and $s \to 0$. For instance, the classical diffusive equation is obtained[28] by choosing p and ψ to be, respectively, a Gaussian (with zero mean and variance σ^2) and exponential pdf (with mean time τ_0). The Gaussian law satisfies that,

$$\hat{p}(k) \sim 1 - \sigma^2 k^2, \quad k \to 0, \tag{6}$$

and the exponential pdf that,

$$\tilde{\psi}(s) \sim 1 - \tau_0 s, \quad s \to 0. \tag{7}$$

This leads to an asymptotic behaviour of the propagator of the form,

$$\bar{G}(k,s) \sim \frac{1}{s + (\sigma^2/\tau_0)k^2}, \quad s \to 0, k \to 0. \tag{8}$$

Inserting this expression into Eq. 3, one can easily reorder terms and get,

$$s\bar{n}(k,s) - \hat{n}_0(k) \simeq -\frac{\sigma^2}{\tau_0} k^2 \bar{n}(k,s) + \bar{S}(k,s), \tag{9}$$

whose Laplace-Fourier inverse becomes the usual diffusive equation:

$$\frac{\partial n}{\partial t} = \frac{\sigma^2}{\tau_0} \frac{\partial^2 n}{\partial x^2} + S(x,t), \quad n(x,0) = n_0(x). \tag{10}$$

It should be noted that, in the purely diffusive case, σ and τ_0 provide the finite characteristic scales for transport. For that reason, one must choose functions for $p(\Delta x)$ and $\psi(\Delta t)$ that respectively lack a finite variance and a finite mean if the intention is to build a transport model for a system in which the dynamics are self-similar and divergent. The same central limit that advises picking Gaussians in many situations, points us now towards strictly stable Lévy distributions $L_{[\alpha,\lambda,\sigma]}(x)$ (see Appendix A), all of which lack a finite variance[30]. The parameter $\alpha \in (0,2)$ determines the tail behaviour of the distribution, that scales as $L(x) \sim |x|^{-(1+\alpha)}$ for large values of the argument. Since $\alpha < 2$, all Lévy pdfs do lack a finite variance as stated (in fact, for $\alpha \leq 1$, they also lack a finite mean!). Next, $\lambda \in [-1,1]$, is a symmetry parameter, with the Lévy law being symmetric (i.e., $L(-x) = L(x), \quad \forall x$) only for $\lambda = 0$. σ, on the other hand, is a shape parameter that measures the width of the distribution in the sense that its finite moments ($p < \alpha$),

$$\langle |x|^p \rangle \coloneqq \int_{-\infty}^{\infty} dx L_{[\alpha,\lambda,\sigma]}(x)|x|^p = c^p_{\alpha,\lambda}(p)\sigma^p, \tag{11}$$

are proportional to powers of σ. The definition of the constant $c_{\alpha,\lambda}(p)$ can be found elsewhere[30]. For symmetric Lévy pdfs (i.e., those with $\lambda = 0$), one can even define an effective width w by means of the expression $w^p \coloneqq \langle |x|^p \rangle$.

In many applications[22], the microscopic transport process is unbiased and symmetric in space, that leads to the natural choice of $p(\Delta x) = L_{\alpha,0,\sigma}(\Delta x)$ as the jump size distribution, for some appropriate values of $\alpha < 2$ and $\sigma > 0$ that must be determined. On the other hand, waiting-times can only be positive and must therefore lack a finite mean if a characteristic scale does not exist. It is thus convenient to choose $\psi(\Delta t) = L_{\beta,1,\tau}(\Delta t)$ as waiting-time pdf, for appropriate $\beta < 1$ and $\tau > 0$. Distributions with $\beta = 1$ are part of a subfamily known as extremal Lévy distributions (see Appendix A), that have the nice property of being defined only for $\Delta t > 0$. Extremal Lévy pdfs also lack a finite mean since they scale as $\psi(\Delta t) \sim \Delta t^{-(1+\beta)}$ for large Δt.

In the case of the running sandpile automaton, however, sand can only travel in one direction: down the slope. Thus, a symmetric Levy pdf would be an inappropriate choice for the jump pdf. Instead, we will choose another extremal distribution, $p(\Delta x) = L_{\alpha,1,\sigma}(\Delta x)$, with $0 < \alpha < 1$ and $\sigma > 0$. This fully asymmetric choice will however lead to a transport equation that is rather different from what is often used in other applications, as it will become apparent very soon. In particular, it is worth to differentiate from other non-symmetric choices sometimes found in the literature, such as the consideration of CTRWs with a drift[31], that are not adequate for the sandpile case examined here.

To proceed with the derivation of the effective transport model, we will need to use two well-known properties of all extremal Levy distributions[30]. Namely, that their Laplace transform behaves as,

$$\tilde{L}_{[\beta,1,\tau]}(s) \sim 1 - \frac{\tau^\beta s^\beta}{\cos(\pi\beta/2)}, \quad s \to 0, \tag{12}$$

and that its Fourier transform behaves, for $k \to 0$, as ($i = \sqrt{-1}$),

$$\hat{L}_{[\alpha,1,\sigma]}(k) \sim 1 - \sigma^\alpha |k|^\alpha \left(1 - \frac{ik}{|k|}\tan\left(\frac{\pi\alpha}{2}\right)\right). \tag{13}$$

Inserting these asymptotic behaviours in the CTRW propagator (Eq. 5), one obtains ($s \to 0, k \to 0$):

$$\bar{G}(k,s) \sim \frac{s^{\beta-1}}{s^\beta + \cos\left(\frac{\pi\beta}{2}\right)\frac{\sigma^\alpha}{\tau^\beta}|k|^\alpha\left(1 - \frac{ik}{|k|}\tan\left(\frac{\pi\alpha}{2}\right)\right)}. \tag{14}$$

The Laplace-Fourier transform of the CTRW general solution (Eq. 3) then becomes, after some straightforward reordering,

$$\begin{aligned} s\bar{n}(k,s) - \hat{n}(k,0) &\simeq \bar{S}(k,s) - \\ &- s^{\beta-1}\left[D_{\alpha,\beta}|k|^\alpha\left(1 - i\frac{k}{|k|}\tan\left(\frac{\pi\alpha}{2}\right)\right)\right]\bar{n}(k,s), \end{aligned} \tag{15}$$

where we have defined a fractional transport coefficient $D_{\alpha,\beta} := \cos(\pi\beta/2)\sigma^\alpha/\tau^\beta$. This equation can be Fourier-Laplace inverted to yield,

$$\frac{\partial n}{\partial t} = {}_0D_t^{1-\beta}\left[D_{\alpha,\beta}\frac{\partial^{\alpha,1}n}{\partial|x|^{\alpha,1}}\right] + S(x,t), \qquad (16)$$

by introducing a Rieman-Liouville fractional derivative (see Appendix B) in time and a Riesz-Feller fractional derivative (see Appendix C) in space. In particular, ${}_0D_t^{1-\beta}$ is a Rieman-Liouville fractional derivative of order $1-\beta$ and start point at $t=0$. On the other hand, $\partial^{\alpha,1}/\partial|x|^{\alpha,1}$ is a completely asymmetrical (and left-sided) Riesz-Feller fractional derivative of order α.

It is at this point where the most meaningful difference with systems in which unbiased, symmetric transport takes place at the microscopic level. In the unbiased case, one usually picks $p(\Delta x) = L_{\alpha,0,\sigma}(\Delta x)$ as the jump size distribution, which leads to the transport equation[28],

$$\frac{\partial n}{\partial t} = {}_0D_t^{1-\beta}\left[D_{\alpha,\beta}\frac{\partial^{\alpha} n}{\partial|x|^{\alpha}}\right] + S(x,t), \qquad (17)$$

that contains the symmetric Reisz operator (Appendix C). As a result, changes in $n(x,t)$ at location x is calculated by collecting the contributions from all locations $x' < x$ and $x' > x$. In contrast, Eq. 16 contains the asymmetrical (left-sided) Reisz-Feller derivative, that is defined as:

$$\frac{\partial^{\alpha,1}n}{\partial|x|^{\alpha,1}} \propto \frac{d^k}{dx^k}\left[\int_{-\infty}^{x}\frac{n(x')dx'}{(x-x')^{\alpha-k+1}}\right], \qquad (18)$$

with k defined as the integer satisfying $k-1 < \alpha < k$. Here, only points $x' < x$ contribute to the integral, a reflection of the fact that net transport can only come from the left (i.e., down the slope, in the running sandpile), and not from the right.

Furthermore, these distinctions imply that some usual associations made in the context of Eq. 17 are no longer true. For instance, it is traditional to define a transport exponent $H = \beta/\alpha$, that quantifies how the finite moments of the propagator of Eq. 17 grow with time:

$$\langle|x-x_0|^p G_{\text{Eq. 17}}(x,t|x_0,0)\rangle \propto t^{pH}, \qquad (19)$$

being x_0 the initial position. For unbiased, symmetric motion, $H > 1/2$ is often referred to as superdiffusive behaviour, whilst $H < 1/2$ is subdiffusive behaviour. These names reflect the fact that the propagator spreads faster or slower than their diffusive counterpart (i.e., $\beta = 1$, $\alpha = 2$). For biased motion, on the other hand, an exponent $H = \beta/\alpha$ could still be defined, but it would make no sense to interpret it in a similar way, since the propagator is now fully asymmetric. Therefore, Eq. 19 no longer characterize how the propagator spreads around its "center of mass", since they will be strongly affected by how fast the "center of mass" itself moves down the slope (which, for symmetric motion, it does not!).

IV. FRACTIONAL EXPONENTS FOR THE RUNNING SANDPILE

In order to use Eq. 16 as a mean field model for transport in the sandpile, we need to estimate first the fractional exponents α and β. There are several ways to do this. One of the simplest ones is to take advantage of the asymptotic behavior of the propagator of the transport equation defined in Eq. 14. In particular, it can be shown that, for fixed t_c, it satisfies that[32]:

$$G(x,t_c|x_0) \sim (x-x_0)^{-(1+\alpha)},\ x - x_0 \gg D_{\alpha,\beta}^{1/\beta}t_c^{\beta/\alpha}. \qquad (20)$$

On the other hand, for fixed $x_c > x_0$, it satisfies that,

$$G(x_c,t|x_0,0) \sim t^{\beta},\ t \ll D_{\alpha,\beta}^{1/\beta}x_c^{\alpha/\beta}, \qquad (21)$$

and,

$$G(x_c,t|x_0,0) \sim t^{-\beta},\ t \gg D_{\alpha,\beta}^{1/\beta}x_c^{\alpha/\beta}. \qquad (22)$$

Therefore, one can estimate α and β by constructing the propagator of transport in the running sandpile and quantifying how it changes at fixed position and time. How can one estimate this propagator, though? In our case, we do it by introducing tracers in the sandpile.

A. Advancing tracers in the running sandpile

The propagator of the CTRW gave the probability of finding a walker at position x and time t after having been at x_0 at time t_0. The propagator of the transport equation, on the other hand, gives the temporal evolution of the initial condition $n(x,0) = \delta(x-x_0)$. Therefore, one can in principle estimate it by following the motion of a sufficiently large number of marked grains of sand (or tracers) that are initially localized very close to each other. In order to do this, we need to consider however a different population of sand grains that, although advanced together with the normal sand, are inert in the sense that they are not considered when a cell is checked for instability. Or, in other words, none of these tracers are considered when updating the local sandpile height or gradient.

Following Ref. 28, we will focus on a narrow strip of width N_f at the sandpile surface, which is the active layer where motion takes place. We will consider N marked grains of sand that will be initially located close to the center of the sandpile. The temporal evolution of the marked population, as it is transported down the pile, will be used to build the propagator we are looking for. The m-th marked grain will be positioned, at some initial time, t_0^m, at an arbitrary cell i_m, chosen randomly from within a reduced number of cells near the top of the pile. The initial position of the m-th grain is then $x_m(0) = i_m$; its depth in the i_m column, as measured from its top, will be initially set to $d^m(0) = uN_f$, where u is a random number uniformly distributed in $[0,1]$. As the

sandpile is iterated, the position, x^m, and depth d^m of the marked grain of sand will change. Their values, at the k-th iteration, will be updated after finding out which of the following rules applies[33]:

1. the current cell is stable and no grains of sand have been dropped on it in the previous driving phase;
   then $d^m(k) = d^m(k-1)$; $x^m(k) = x^m(k-1)$;

2. the current cell is stable, but N_b grains of sand have fallen on it in the previous driving phase;
   then $d^m(k) = d^m(k-1) + N_b$; $x^m(k) = x^m(k-1)$;

3. the current cell is stable, but the previous one is unstable and moves N_f grains over to the current cell;
   then $d^m(k) = d^m(k-1) + N_f$; $x^m(k) = x^m(k-1)$;

4. the current cell is stable, the previous one is unstable and, in the driving phase, N_b grains have fallen on the current cell;
   then $d^m(k) = d^m(k-1) + N_f + N_b$; $x^m(k) = x^m(k-1)$;

5. the current cell is unstable and N_f grains are thus moved to the following cell; no grains of sand have been dropped on the current cell in the driving phase;
   then, if $d^m(k-1) \leq N_f \longrightarrow d^m(k) = uN_f$;
   $x^m(k) = x^m(k-1) + 1$;
   if $d^m(k-1) > N_f \longrightarrow d^m(k) = d^m(k) - N_f$;
   $x^m(k) = x^m(k-1)$;

6. the current cell is unstable and N_f grains are thus moved to the following cell; at the previous driving phase, N_b grains of rain have fallen on the current cell;
   then, if $d^m(k-1) \leq N_f - N_b \longrightarrow d^m(k) = uN_f$;
   $x^m(k) = x^m(k-1) + 1$;
   if $d^m(k-1) > N_f - N_b \longrightarrow d^m(k) = d^m(k) - N_f + N_b$;
   $x^m(k) = x^m(k-1)$;

The majority of these rules are rather self-explanatory. Basically, they state that, when it is time to move N_f particles to the next cell, our marked grain will be transported together with that bunch only if its depth in the cell is at most N_f. In that case, the marked grain of sand will reset its depth at the new cell to a new value, randomly chosen between 0 and N_f since u is a random number uniformly distributed in $[0, 1]$. If the marked grain is however deeper than N_f, it remains at the current cell. In the (relatively rare) case that sand has been dropped during the previous driving phase on the same cell where the marked grain sits, the depth of the marked grain is increased by N_b.

Fig. 4 shows the motion across the sandpile (size $L = 10000$, critical slope $Z_c = 200$, toppling size $N_f = 30$, rain probability $p_0 = 10^{-4}$ and rain size $N_b = 1$) of ten marked grains of sand for the first 10^6 iterations. As can be appreciated, the grains alternate radial displacements when carried by a passing avalanche −that appear as nearly horizontal segments (in fact, they are not exactly horizontal since particles advance one position per iteration. However, the scale of the temporal axis used in the figure makes them look so)−, with periods of rest at the same cell, while the grain remains trapped there −that appear as vertical segments.

B. Propagator estimation in the running sandpile

The recorded positions of the marked grains of sand can be used to build a discrete version of the sandpile propagator. All that is needed is to calculate, at each iteration, the pdf of the particle displacements with respect to their respective initial locations, $p(\Delta x; k)$. By using relative displacements (from each initial location), we can seed many more marked grains than the N_f that would fit within the active narrow layer at a single location. We can now initialize up to N_f of them at as many cells as desired, which greatly improves the statistics. It must be said, though, that by doing so we have implicitly assumed that all these cells have similar dynamics. This is, to a great extent, the case for the running sandpile due to the uniformly spread random drive. Each marked grain will contribute with the displacement value $\Delta x^m(k) = x^m(k) - x^m(0)$ $(m = 1, \cdots, N)$ at iteration k. Since $p(\Delta x; k)$ thus gives the probability of a particle having been displaced a distance Δx in a time k, averaged over its initial location, we can write that,

$$p(\Delta x; k) \simeq \langle G(x_0 + \Delta x, k | x_0, 0) \rangle_{x_0} , \qquad (23)$$

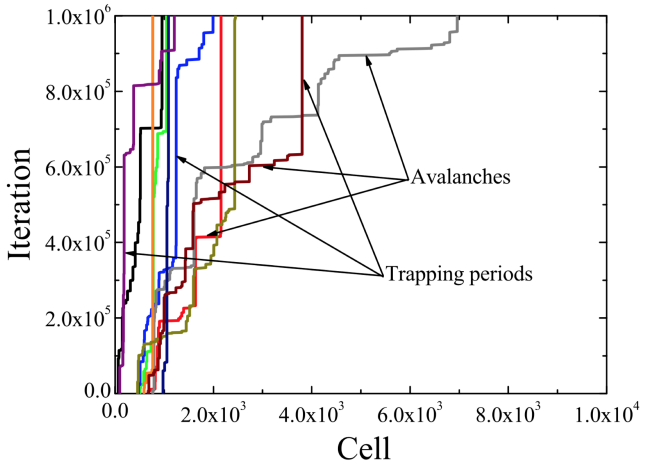

FIG. 4: (Color online) Motion across the sandpile of size $L = 10000$ of ten selected particles, with initial locations randomly chosen within the central half of the pile. The vertical parts of the trajectories correspond to periods in which the particle is at rest on some cell; the (almost) horizontal parts, to periods of time in which the particle is transported radially, carried away by passing avalanches.

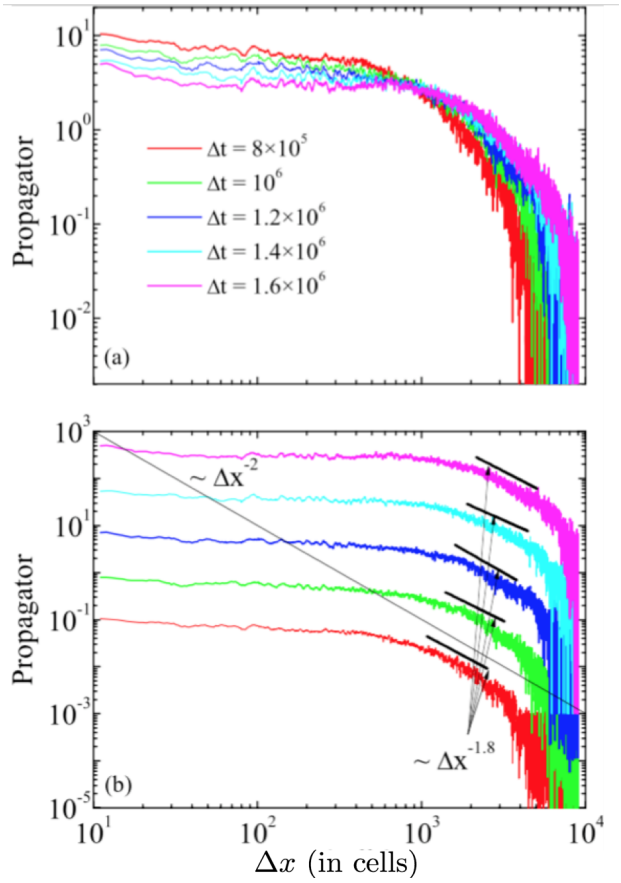

FIG. 5: (Color online) (a) Sandpile propagator for times corresponding to $(0.8, 1.0, 1.2, 1.4 \text{ and } 1.6) \times 10^6$ iterations using 10000 tracer particles for the $L = 10000$ sandpile with $Z_c = 200$, $N_f = 30$, $N_b = 1$ and $P_0 = 10^{-4}$. In (b), the same propagators have been shifted to better appreciate the power-law regions scaling as $P(\Delta x) \sim \Delta x^{-1.8}$. The algebraic scaling Δx^{-2} is also shown (in black) to guide the eye.

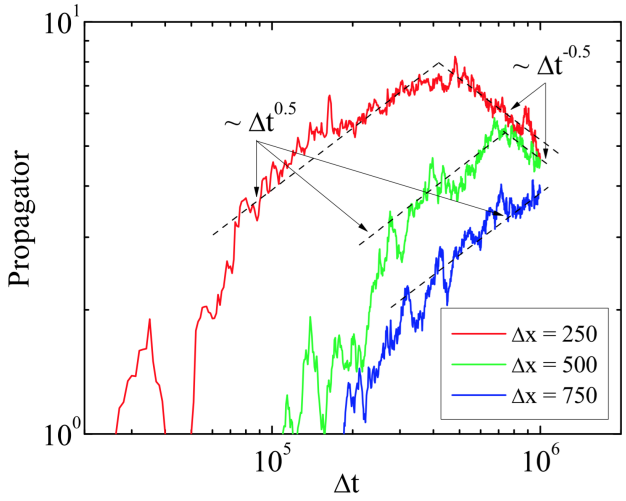

FIG. 6: (Color online) Estimate of the evolution of the sandpile propagator at fixed positions, $\Delta x = 250$, $\Delta x = 500$ and $\Delta x = 750$, as a function of time using 10000 tracer particles for the $L = 10000$ sandpile with $Z_c = 200$, $N_f = 30$, $N_b = 1$ and $P_0 = 10^{-4}$. As expected, the local value first grows and then decays algebraically as $P(\Delta t) \sim \Delta t^{\pm 0.5}$.

which is the estimate of the propagator of the running sandpile we are looking for.

There are some limitations that must be however considered while estimating the propagator in this way. They are due to the unavoidable fact that each marked grain does eventually reach the end of the sandpile. Therefore, Eq. 23 should not be used beyond the typical number of iterations required for the closest marked particles to reach the pile edge. In addition, one also needs to consider that, since marked grains have been initialized at different locations in order to improve statistics, each one travels a different distance to reach the edge of the sandpile. To avoid possible distortions, contributions to Eq. 23 from any Δx larger than the minimum of these distances should also be disregarded.

Fig. 5(a) shows snapshots of the sandpile propagator obtained at different times using $N = 10000$ marked grains, that were uniformly initialized at cells with $x^m(0) \leq x_{\max} = L/10 = 1000$ for any tracer $m \in [1, N]$ (note that $L = 10000$ for all these simulations). In Fig. 5(b) the same propagators have been shifted up (magenta and cyan) and down (red and green) to better appreciate the power-law regions where the corresponding fits have been performed. The propagators exhibit power law regions beyond certain displacement values, that are eventually replaced by exponential cutoffs due to finite-size effects. In particular, power-law scalings close to $p(\Delta x) \sim \Delta x^{-1.8}$ are apparent that become distorted at times of the order of 10^6 iterations and above. This number is of the order of the number of iterations required for a sizable amount of marked particles to have reached the sandpile edge. By using Eq. 20, we can thus infer a value $\alpha \sim 0.8$ for the spatial fractional exponent of the effective fractional transport model (Eq. 16) for the running sandpile.

We estimate next the temporal fractional exponent by quantifying the initial growth (Eq. 21) and later decay (Eq. 22) of the propagator at a fixed location. In Fig. 6, its temporal evolution is shown at three different fixed displacement values, $\Delta x = 250$, $\Delta x = 500$ and $\Delta x = 750$. For the smallest displacement, the propagator grows as $p(\Delta t) \sim \Delta t^{0.5}$ for $\Delta t < 4 \times 10^5$, and then decreases as $p(\Delta t) \sim \Delta t^{-0.5}$ for $\Delta t > 4 \times 10^5$. For $\Delta x = 500$, the propagator grows as $p(\Delta t) \sim \Delta t^{0.5}$ but for time lapses lasting double, $\Delta t < 8 \times 10^5$. Then decreases also as $p(\Delta t) \sim \Delta t^{-0.5}$ for $\Delta t > 8 \times 10^5$. Finally, for the largest displacement, the decay phase is however not seen within the 10^6 iterations considered. In fact, it would take approximately 1.6×10^6 iterations to appreciate the beginning of this phase for this displacement. Therefore, from Eqs. 21 and 22 we can infer a value $\beta \sim 0.5$ for the temporal exponent of the effective fractional transport model (Eq. 5) for the running sandpile.

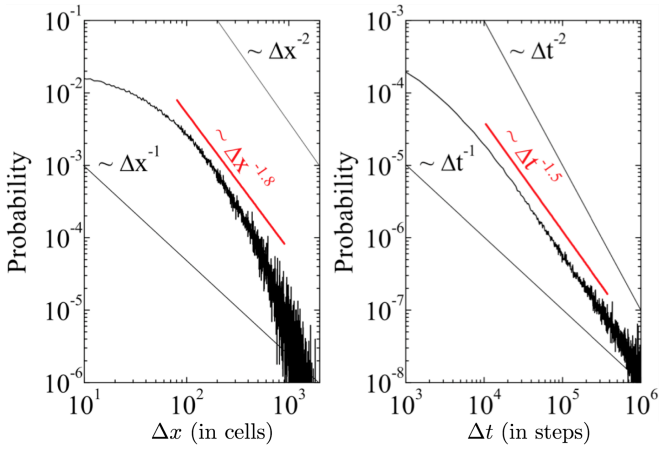

FIG. 7: (Color online) Probability density functions for the jump sizes (left) and waiting times (right) of marked grains of sand moving across a running sandpile $L = 10000$ sandpile with $Z_c = 200$, $N_f = 30$, $N_b = 1$ and $P_0 = 10^{-4}$.

In order to increase our confidence in these exponent values, we have also estimated the pdfs of waiting-times and jump sizes of the marked grains directly. To do it, we have considered the (almost) horizontal marker displacements in Fig. 4 as the instantaneous jumps, and the vertical segments as waiting times. Their pdfs are shown in Fig. 7. As can be seen, $p(\Delta x) \sim \Delta x^{-1.8}$ over sufficiently large values, before the appearance of the unavoidable exponential cutoff at the largest scales; on the other hand, $\psi(\Delta t) \sim \Delta t^{-1.5}$ over the mesorange scales. Therefore, these pdfs are consistent with the values $\alpha \sim 0.8$ and $\beta \sim 0.5$ that were obtained from the propagator analysis.

V. DISCUSSION

In the previous section, we have found that the long-range, large-scale features of transport across the running sandpile seem to be well modelled by Eq. 16 with $\alpha \sim 0.8$ and $\beta \sim 0.5$. The range of lengthscales over which the exponent α is well defined is, roughly, $\Delta x \in \left[10^2 - 10^3\right]$, well separated from the minimum (1) and maximum (10000) sizes allowed in the sandpile ($L = 10000$), where finite size effects are expected. The range of timescales over which β is well defined is longer, roughly $\Delta t \in \left[10^4 - 10^6\right]$. That is, much longer than the maximum duration avalanches can have in the sandpile, which is of the order of L. This suggests that the fact that exponent β is significantly smaller than 1 is needed to capture the long-term persistence that is associated to the evolution of the roughness of the sandpile height profile. Or, in other words, to the influence of the footprints left behind by previous avalanches on the future transport across the sandpile.

Another interesting point regards the aforementioned transport exponent, $H = \beta/\alpha$. As we mentioned previously, this transport exponent is often used when discussing symmetric transport[15,28]. Indeed, $H = 0.5$ is usually called a diffusive scaling, whilst $H > 0.5$ is referred to as superdiffusion, and $H < 0.5$, as subdiffusion. In the running sandpile, however, this interpretation is meaningless since the propagator for Eq. 16 is not only asymmetric, but fully biased towards the down-the-slope direction. Therefore, although one could still estimate this transport exponent to be $H \sim 0.62$, its value cannot be interpreted as indicative of superdiffusive transport taking place across the running sandpile. Indeed, H no longer quantifies how the propagator spreads with respect to its "center of mass" (as it does for symmetric motion), but how fast the "center of mass" moves down the slope (which, in a symmetric case, it does not!).

Finally, we would like to make some comments regarding the practical use of Eq. 16 as an effective model for the running sandpile. The first comment is that the starting point of the spatial integral in Eq. 16 must be replaced by 0, the innermost sandpile position (or one could assume that $n(x,t) = 0, \forall x < 0$, at all times). Secondly, the kernel of the Riesz-Feller integral might then need to be regularized to avoid a possible divergence of the fractional derivative at its starting point, $x = 0$, that might appear when imposing initial/boundary conditions expressed in terms of usual (i.e., integer) derivatives[34], as often happens in physical systems (see Appendix B). The regularization of fractional derivatives is a relatively standard practice in most applications of fractional transport equations. Many details about these procedures can be found in the literature[23].

VI. CONCLUSIONS

In this work, we have constructed an effective model for transport across the running sandpile cellular automaton based on fractional derivatives. The resulting transport equation (Eq. 16) must be written in terms of fully asymmetric fractional derivatives both in space and time, due to the fully biased nature of sand motion in the sandpile, that only takes place down the slope. This is in contrast with more common applications of fractional transport equations, that often describe systems in which unbiased, symmetric motion takes place, resulting in the use of symmetric fractional derivatives in space. This difference forces us to revise the interpretation of some of the exponents that characterize the model. We have also estimated the fractional exponents required to complete the effective model by using marked grains of sand as a diagnostic tool. We expect that this exercise might serve as a guide to address similar problems in more complicated systems such as, for example, the construction of reliable effective transport models for the radial transport of energy and particles out of fusion plasmas confined in tokamaks in near-marginal regimes[15].

Acknowledgments

This research has been sponsored in part by Ministerio de Economía y Competitividad of Spain under Projects No. ENE2015-68265-P and No. ENE2015-66444-R. Research also supported in part by DOE-OFES Grant No. DE-FG02-04ER5741 at University of Alaska. This work has also been carried out within the framework of the EUROfusion Consortium and has received funding from the Euratom research and training programme 2014-2018 under grant agreement No 633053 for the project WP17-ER/ENEA-10. The views and opinions expressed herein do not necessarily reflect those of the European Commission. Sandpile automata simulations have been run in *Uranus*, a supercomputer cluster at Universidad Carlos III de Madrid (Spain) that has been funded by the Spanish Government via the national projects UNC313-4E-2361, ENE2009-12213-C03-03, ENE2012-33219 and ENE2012-31753. Fruitful interactions with members of the ABIGMAP research network, funded by the Spanish Project MAT2015-69777-REDT, are also acknowledged.

Appendix A: stable Lévy distributions

The Lévy family of pdfs comprises all the limit distributions that are strictly stable with respect to the sum of N independent and identically distributed random variables[30]. They can be defined in closed form only via their characteristic function (or Fourier transform):

$$L_{[\alpha,\lambda,\sigma]}(k) = \exp\left\{-\sigma^\alpha |k|^\alpha \left[1 - \frac{i\lambda k}{|k|}\tan\left(\frac{\pi\alpha}{2}\right)\right]\right\}, \tag{24}$$

with the parameters varying in $\alpha \in (0,2]$, $|\lambda| \leq 1$ and $\sigma > 0$. Here, $i = \sqrt{-1}$.

Meaning of parameters.- Each parameter has a very different meaning. First, $|\lambda| \leq 1$ measures the asymmetry of the distribution since[30],

$$L_{[\alpha,\lambda,\sigma]}(y) = L_{[\alpha,-\lambda,\sigma]}(-y). \tag{25}$$

If $\lambda = 0$, the pdf is symmetric (and, for $\alpha = 1, 2$, it is the only possible value). Secondly, α characterizes the tail behaviour of the pdf. For $\alpha \neq 1$, it happens that[30],

$$L_{[\alpha,\lambda,\sigma]}(y) \sim \begin{cases} C_\alpha \left(\frac{1-\lambda}{2}\right) \sigma^\alpha |y|^{-(1+\alpha)}, & y \to -\infty \\ C_\alpha \left(\frac{1+\lambda}{2}\right) \sigma^\alpha |y|^{-(1+\alpha)}, & y \to +\infty \end{cases}, \tag{26}$$

with the constant given by:

$$C_\alpha = \frac{\alpha(\alpha-1)}{\Gamma(2-\alpha)\cos(\pi\alpha/2)}, \tag{27}$$

being $\Gamma(x)$ the usual Gamma function. In the special case $\alpha = 1$, the Lévy pdf (known as a Cauchy pdf) decays as $L_{[1,0,\sigma]}(y) \sim (\sigma/\pi)|y|^{-2}$. Finally, σ is the scale parameter because[30],

$$L_{[\alpha,\lambda,\sigma]}(ay) = L_{[\alpha,\mathrm{sgn}(a)\lambda,|a|\sigma]}(y). \tag{28}$$

Extremal Lévy distributions.- A Lévy distribution is called *extremal* if $\lambda = \pm 1$ [This can only happen for $\alpha \neq 1, 2$.]. According to Eq. 26, the power-law decay is only observed for one of the two tails (for positive or negative y's) depending on the sign of λ, with the other tail decaying exponentially fast. Indeed, for $1 < \alpha < 2$, $\lambda = \pm 1$ forces the tail for $y \to \mp\infty$ to decay exponentially. For $0 < \alpha < 1$ the extremal distribution becomes one-sided[30]. That is, they are defined only for $y > 0$ if $\lambda = +1$, and for $y < 0$ if $\lambda = -1$. In that case, the exponential tail is found in the limit $y \to 0\pm$ for $\lambda \to \mp 1$. A useful property of extremal Lévy distributions is that its Laplace transform is given by:

$$\tilde{L}_{[\alpha,1,\sigma]}(s) = \exp\left(-\frac{\sigma^\alpha}{\cos(\pi\alpha/2)} s^\alpha\right). \tag{29}$$

Appendix B: Riemann-Liouville fractional derivatives

Riemann-Lioville (RL) fractional derivatives are integro-differential operators that provide interpolants between derivatives of integer order[34].

Riemann-Liouville fractional derivatives.- The left-sided RL fractional derivative of order $p > 0$ of a function $f(t)$ is defined as[34]:

$${}_aD_t^p f(t) \equiv \frac{1}{\Gamma(k-p)} \frac{d^k}{dt^k} \int_a^t (t-\tau)^{k-p-1} f(\tau) d\tau, \tag{30}$$

where the integer k satisfies that $k - 1 \leq p < k$. For $p = n$, the RL fractional derivative reduces to the standard derivative of order n. Right-sided RL fractional derivatives can also be defined:

$${}^bD_t^p f(t) \equiv \frac{1}{\Gamma(k-p)} \frac{d^k}{dt^k} \int_t^b (\tau-t)^{k-p-1} f(\tau) d\tau. \tag{31}$$

Their properties are analogous to the left-sided counterpart.

RL fractional derivatives have interesting, but somewhat not intuitive properties. The most striking property is probably that the fractional derivative of a constant function is not zero. Indeed, using the fact that the derivative of a power law can be calculated to be[30] ($p > 0$, $\nu > -1$, $t > 0$):

$${}_aD_t^p \cdot (t-a)^\nu = \frac{\Gamma(1+\nu)}{\Gamma(1+\nu-p)} (t-a)^{\nu-p}, \tag{32}$$

it is clear that choosing $\nu = 0$ does not yield a constant, but $(t-a)^{-p}/\Gamma(1-p)$.

RL fractional derivatives can be combined with other derivatives (fractional or integer). But the combinations are not always simple. For instance, the action of normal derivatives on RL fractional derivatives is:

$$\frac{d^m}{dt^m} \cdot {}_aD_t^p f(t) = {}_aD_t^{p+m} f(t). \tag{33}$$

For the right side RL derivatives, this property becomes:

$$(-1)^m \frac{d^m}{dt^m} \cdot {}^b D_t^p f(t) = {}^b D_t^{p+m} f(t). \tag{34}$$

However, the action of the RL fractional derivative on a normal derivative is much more complicated[30].

Relatively simple expressions exist for the Laplace transform of the left-sided RL fractional derivative of order p, if the starting point is $a = 0$:

$$L\left[{}_0D_t^p \cdot f(t)\right] = s^p \tilde{f}(s) - \sum_{j=0}^{k-1} s^j \left[{}_0D_t^{p-j-1} \cdot f(t)\right]_{t=0}. \tag{35}$$

This expression is very reminiscent of the one for normal derivatives. Similarly, the Fourier transform of the left-sided RL fractional derivative satisfies a very simple relation when the starting point is $a = -\infty$:

$$\mathrm{F}\left[{}_{-\infty}D_t^p \cdot f(t)\right] = (i\omega)^p \, \hat{f}(\omega). \tag{36}$$

For the right-sided fractional integral with ending point $b = \infty$, the Fourier transform satisfies:

$$\mathrm{F}\left[{}^{\infty}D_t^p \cdot f(t)\right] = (-i\omega)^p \, \hat{f}(\omega). \tag{37}$$

Finally, it is worth mentioning that the left[right]-sided fractional derivative of a function $f(x)$ may exhibit a divergence at their start[end] point when one prescribes the values of this function or its integer derivatives at the start[end] point (as it is often done in many applications, where initial value or boundary value problems often appear). This can be made apparent, for instance, by calculating the fractional derivative of a regular function by means of its Taylor expansion. In the case in which $0 < \alpha < 1$, it becomes[23]:

$$\begin{aligned} {}_aD_t^\alpha f(x) = \quad & \frac{1}{\Gamma(1-a)} \frac{f(a)}{(x-a)^\alpha} + \\ & + \sum_{k=0}^{\infty} \frac{f^{(k+1)}(a)}{\Gamma(k+2-\alpha)} (x-a)^{k+1-\alpha} \end{aligned} \tag{38}$$

This expression is clearly divergent at $x = a$ if $f(a) \neq 0$. A similar expression can be obtained for $1 < \alpha < 2$. In that case,

$$\begin{aligned} {}_aD_t^\alpha f(x) = \quad & \frac{1}{\Gamma(1-a)} \frac{f(a)}{(x-a)^\alpha} + \\ & + \frac{1}{\Gamma(2-a)} \frac{f'(a)}{(x-a)^{\alpha-1}} + \\ & + \sum_{k=0}^{\infty} \frac{f^{(k+2)}(a)}{\Gamma(k+3-\alpha)} (x-a)^{k+2-\alpha} \end{aligned} \tag{39}$$

that is divergent at $x = a$ if either $f(a) \neq 0$ or $f'(a) \neq 0$. These divergences can be avoided if one prescribes the values of fractional derivatives of the function at the start[end] point instead. However, this is usually difficult to justify physically in most situations[34]. For that reason, regularization techniques are often used to avoid these divergences in practical applications, as it has been widely described in the literature[23] .

Appendix C: The Riesz-Feller fractional derivatives

The Riesz fractional derivative of order α is defined by the integral:

$$\frac{\partial^\alpha f}{\partial |x|^\alpha} \coloneqq -\frac{1}{2\Gamma(\alpha)\cos(\alpha\pi/2)} \int_{-\infty}^{\infty} dx' \frac{f(x')}{|x-x'|^{\alpha+1}}. \tag{40}$$

The most remarkable property of this derivative has to do with its Fourier transform, that satisfies[35]:

$$\mathrm{F}\left[\frac{\partial^\alpha f}{\partial |x|^\alpha} \right] = -|k|^\alpha \hat{f}(k). \tag{41}$$

Using now the complex identity ($i = \sqrt{-1}$),

$$(ik)^\alpha + (-ik)^\alpha = 2\cos\left(\frac{\pi\alpha}{2}\right) |k|^\alpha, \tag{42}$$

it is very easy to prove that the Riesz derivative can also be expressed as a symmetric sum of two RL fractional derivatives (one left-sided, one right-sided) of order α[30],

$$\frac{\partial^\alpha f}{\partial |x|^\alpha} = -\frac{1}{2\Gamma(\alpha)\cos(\alpha\pi/2)} \left[{}_{-\infty}D_x^\alpha + {}^{\infty}D_x^\alpha \right]. \tag{43}$$

An asymmetric version of the Riesz-Feller derivative also exists[36]. It is often referred to as the Riesz-Feller fractional derivative of order α with asymmetry parameter $|\lambda| \leq 1$. It is more easily defined through its Fourier transform, that is:

$$\mathrm{F}\left[\frac{\partial^{\alpha,\lambda} f}{\partial |x|^{\alpha,\lambda}} \right] = -|k|^\alpha \left[1 - i\lambda \frac{|k|}{k} \tan\left(\frac{\alpha\pi}{2}\right) \right] \hat{f}(k). \tag{44}$$

For $\lambda = 0$, the standard symmetric Riesz derivative is recovered. The asymmetric Riesz-Feller derivative can also be expressed as an asymmetric sum of two RL fractional derivatives of order α[37]:

$$\begin{aligned} \frac{\partial^{\alpha,\lambda} f}{\partial |x|^{\alpha,\lambda}} = & -\frac{1}{2\Gamma(\alpha)\cos(\alpha\pi/2)} \cdot \\ & \cdot \left[c_-(\alpha,\lambda) {}_{-\infty}D_x^\alpha f + c_+(\alpha,\lambda) {}^{\infty}D_x^\alpha f \right], \end{aligned} \tag{45}$$

with the $c_\pm$ coefficients being defined as:

$$c_\pm(\alpha,\lambda) \coloneqq \frac{1 \mp \lambda}{1 + \lambda\cos\left(\frac{\alpha\pi}{2}\right)}. \tag{46}$$

Thus, in the limit of $\lambda = 1$, only the left-sided RL derivative ${}_{-\infty}D_x^\alpha$ remains, whilst for $\lambda = -1$, only the right-side RL derivative ${}^{\infty}D_x^\alpha$ does.

[1] P. Bak, C. Tang and K. Wiesenfeld, *Phys. Rev. Lett.* **59**, 381 (1987).
[2] E. T. Lu and R. J. Hamilton, *Astroph. J.* **380**, L89 (1991).
[3] B. E. Shaw, J. M. Carlson and J. S. Langer, *J. Geoph. Res.* **97**, 479 (1992).
[4] B. Drossel and F. Schwabl, *Phys. Rev. Lett.* **69**, 1629 (1992).
[5] P. Bak and K. Sneppen, *Phys. Rev. Lett.* **71**, 4083 (1993).
[6] S. Mineshige, M. Takeuchi and H. Nishimori, *Astroph. J.* **435**, L125 (1994).
[7] T. Nagatani, *Physica A* **218**, 1 (1995).
[8] S. Field, J. Witt, F. Nori and X. Ling, *Phys. Rev. Lett.* **74**, 1206 (1995).
[9] S. Nagel, *Rev. Mod. Phys.* **64**, 321 (1992)
[10] J. Feder, *Fractals* **3**, 431 (1995)
[11] L. P. Kadanoff, S. R. Nagel, L. Wu and S.-M. Zhou, *Phys. Rev. A* **39**, 6524 (1989).
[12] T. Hwa and M. Kardar, *Phys. Rev. A* **45**, 7002 (1992).
[13] D. E. Newman, B. A. Carreras, P. H. Diamond and T. S. Hahm, *Phys. Plasmas* **3**, 1858 (1996).
[14] R. Sanchez, D. E. Newman and B. A. Carreras, *Nucl. Fusion* **41**, 247 (2001).
[15] R. Sanchez and D. E. Newman, *Plasma Phys. Contr. Pus.* **57**, 123003 (2015).
[16] P. H. Diamond and T. S. Hahm, *Phys. Plasmas* **2**, 3640 (1995).
[17] B. A. Carreras et al., *Phys. Plasmas* **3**, 2903 (1996).
[18] E. J. Doyle et al., *Nucl. Fusion* **47**, S18 (2007).
[19] B. A. Carreras, V. E. Lynch and G. M. Zaslaysky, *Phys. Plasmas* **8**, 5096 (2001).
[20] B. Ph. van Milligen, R. Sanchez and B. A. Carreras, *Phys. Plasmas* **11**, 2272 (2004).
[21] D. del-Castillo-Negrete, B. A. Carreras and V. E. Lynch, *Phys. Plasmas* **11**, 082308 (2004)
[22] R. Sanchez, B. A. Carreras and B. Ph. van Milligen, *Phys. Rev. E* **71** 011111 (2005)
[23] D. del-Castillo-Negrete, *Phys. Plasmas* **13**, 082308 (2006).
[24] M. V. Medvedev and P.H. Diamond, *Phys. Rev. E* **58**, 6824 (1998).
[25] J. A. Mier, R. Sanchez and D. E. Newman, *Phys. Rev. E* **94**, 022128 (2016).
[26] R. A. Woodard et al., *Physica A* **373**, 215 (2007).
[27] E. W. Montroll and G. Weiss, *J. Math. Physics* **6**, 167 (1965).
[28] R. Metzler and J. Klafter, *Phys. Reports* **339**, 1 (2000).
[29] M.M. Meerschaert and P. Straka. *Annals of Probability* **42** 1699 (2014)
[30] G. Samorodnitsky and M. S. Taquu. *Stable non-Gaussian random processes*. Chapman & Hall, New York (1994).
[31] M. M. Meerschaert and A. Sikorskii. *Stochastic Models for Fractional Calculus*. De Gruyter, Berlin (2012).
[32] A. Saichev and G. M. Zaslaysky, *Chaos* **7**, 753 (1997).
[33] B. A. Carreras, V. E. Lynch, D. E. Newman and G. M. Zaslavsky, *Phys. Rev. E* **60**, 4770 (1999).
[34] I. Podlubny. *Fractional Differential Equations*. Academic Press, New York (1998).
[35] S. G. Samko, A. A. Kilbas and O. I. Marichev. *Fractional Integrals and Derivatives: Theory and Applications*. Gordon and Breach Eds., New York (1993).
[36] W. Feller. *Introduction to probability theory and applications*. Wiley, New York (1968).
[37] R. Gorenflo et al., *Chemical Physics* **284**, 521 (2002).

Reply to the referee review on the manuscript: "Modelling transport across the running sandpile by means of fractional transport equations", by R. Sanchez et al

We would like to thank the referee for his/her interest in our paper and for the time he/she might have devoted to reading it. In what follows, we provide separate and detailed answers to the referee's comments (marked in bold+italics). We have tried to comply with all the requests made by the referee as much as possible, as reflected in the following paragraphs.

Replies to the referee's comments.-

This paper mainly discusses the running sandpile model. The model and the way of simulations are given. Comparing with the CTRW model, this paper gives the "waiting time"and "jumping length" distributions and some specific constants are confirmed by the numerical simulations. Some simulation results are also given. Our main concern is the effectiveness of the simulation model for real sandpile running? Please give some illustrations. Please also show the effectiveness of Eq. (14) for real sandpile running.

We are afraid that there is a confusion here. The purpose of our paper is not to propose an effective transport model for a "real running sandpile". In fact, it was proved long ago [see, for instance, the papers by S. Nagel, Rev. Mod. Phys. **64**, 321 (1992) or J. Feder, Fractals **3**, 431 (1995)] that a proper modelling of real running sandpiles would require the inclusion of a certain degree of "stickiness" between sand grains that is completely absent in the cellular automata studied here, and that would lead to very different dynamics.

Instead, here we use the running sandpile cellular automata as a proxy to study self-organized critical dynamics in conservative, one-dimensional systems in which directed transport is switched on/off locally by means of a local threshold. This is how this automata has been used in many scientific contexts and, in particular, in the context of fusion plasmas which is our field of expertise. Magnetically-confined plasmas in tokamaks and stellarators have these properties, which is why the running sandpile automata has been studied so much in this area (see, for instance, D.E. Newman et al, Phys. Plasmas **3**, 1858 (1996), S. Chapman et al, Phys. Rev. Lett. **86** 2814 (2001), R. Sanchez et al, Nuclear Fusion **41**, 247 (2001), I. Gruzinova et al, Phys. Rev. Lett. **89**, 255001 (2002) or H. Isliker et al, Phys. Plasmas **17** 082303 (2010).]. In this paper, we use this cellular automata as a testbed in which we look for the kind of fractional transport model that would be more adequate to describe transport phenomenlogicaly in this type of systems, with the idea of then using some of this newly generated knowledge to build effective transport models for radial turbulent transport in tokamaks (other authors could also use it in other systems) in the near future. We have added a few sentences to the introduction to clarify this point and to avoid misguiding readers.

Some revisions are needed.

1. **Page 2. There are 2 points needing to be clarified: one is $N_f > P_0 N_b L$ in the first paragraph in Section 2; the other is $Z \simeq -(Z_c - N_f/2)$. Please make detailed descriptions.**

   The two points raised by the referee have the following explanation. $P_0 N_b L$ is the amount of sand

that is added to the system in each iteration (on average). The system can remove at most N_F in one iteration, when the edge cell becomes unstable. Thus, requiring $N_F > P_0 N_b L$ simply ensures that the sandpile is not overdriven (on average). That is, it could safely remove more sand than is added if needed. Secondly, the average slope in the sandpile at steady state is not $-Z_c$, but it is closer to $-(Z_c - N_F/2)$. The reason is that any time the local slope reaches $-Z_c$, a toppling takes place that brings it down to $-(Z_c - N_F)$. Then, the local slope builds up again towards $-Z_c$ at an average constant rate due to the falling sand rain, process that is only disturbed by passing avalanches. The mid-point between these two values is -$(Z_c - N_F/2)$, that approximates very well what is observed in the simulation. This has been better explained in the resubmitted manuscript.

2. **Page 2. Basing on the Ref. [28], we don't think the model introduced in section 2 is very clear. Could you please polish it?**

   We have extended the description of the running sandpile model in the resubmitted text. The reason why we did not give more details is, simply, that is an old model (first presented in T. Hwa et al, Phys. Rev A **45** 7002 (1992), that is relatively well known in the community.

3. **Page 3. We think there are some mistakes in the Eq. (2). Because the Levy process is no longer a Markov process, and we can't obtain Eq. (14) simply basing on Eq. (2). Please check.**

   There is no mistake in the derivation of Eq. (14), except for the improper use of the word "limit" that the referee also pointed (see item No. 4). The referee could check, for instance, the paper by Montroll [E.W. Montroll et al, J. Math. Phys **6**, 167 (1965)] to find the specific details regarding the solution of the propagator of the CTRW (i.e., our Eq. (4)). In the case of a symmetric Lévy being the choice for $p(\Delta x)$, the derivation of the asymptotic transport equation (analogous to our Eq. 14) can be found, for instance, in R. Metzler et al, Phys. Rep. **339**, 1 (2000). In that case, the resulting spatial fractional operator is the symmetric Riesz derivative. The novelty of our derivation is that we assume instead an extremal, asymmetric Lévy for $p(\Delta x)$, which is a more adequate choice for a system in which transport only takes place in one direction, down the slope.

4. **Page 3 and 4. Both of Eq. (6) and Eq. (12) have the same problem, which the authors might mean the asymptotic behaviours instead of taking limit. So from this point of view, we think it is more suitable if the expression of Eq. (6) and Eq. (12) is changed to** $G(k,s) \sim 1/(s+(\sigma^2/\tau_0)k2)$ **and** $G(k,s) \sim s^{\beta-1}/(s^\beta + \cos(\pi\beta/2)(\sigma^\alpha/\tau^\beta)|k|^\alpha(1-\imath k/|k|\tan(\pi\alpha/2))$**, respectively.**

   The referee is correct in this case. We have thus replaced "limit" by "asymptotic behaviour" in these expressions as well as throughout the text.

5. **Page 4. The last paragraph above section 4. We think whether the process is symmetric or not has no influence on whether the process is diffusion or not. Besides we don't quite understanding the last sentence, we think the p-th moment always means how the propagator spreads around its ?center of mass? (the average we guess) while the asymmetric process only causes the average isn't** 0 **anymore.**

   For the macroscopic motion to be purely diffusive, it is required that the underlying CTRW satisfies that $p(k) \sim 1 - D_0 k^2$ and $\psi(s) \sim 1 - \tau_0 s$. However, if $p(\Delta x)$ is not symmetric, then it will happen that $p(k) \sim 1 + \imath\mu k - D_0|k|^2$ (assuming that all moments are finite), with μ being related to a drift velocity. It is only when $\mu = 0$ that the moments $\langle (x - x_0)\rangle^{2p}$ that we use characterize the spreading of the propagator around its center of mass. This is because x_0 **is the initial position of the particle** (not its average position as a function of time!) and the moments thus also contain

he effect of the drift. Things are more complicated in the case in which $p(\Delta x)$ is a Lévy pdf. But in the symmetric case when $p(k) \sim 1 - D|k|^\alpha$, it remains true that the moments $\langle (x - x_0) \rangle^{2p}$ still give information about the spreading of the propagator. If the motion is not symmetric, this is no longer true as in the case of the standard diffusive case.

6. **Page 8. The last paragraph above section 6. We don?t know why $n(x,t)$ is divergent at the starting point, $x = 0$. Could you please give some detailed explanation about this?**

   Fractional derivatives may diverge at their starting or ending point (depending on whether they are left-sided or right-sided) when these are finite (i.e., not $\pm\infty$).One can calculate the left-sided Riemann-Liouville fractional derivative of order $0 < \alpha < 1$ (this is the derivative that appears in the asymmetric Riesz-Feller derivative of order α) of a regular function $f(x)$ by means of its Taylor expansion to get:

$$ {}_aD_t^\alpha f(x) = \frac{1}{\Gamma(1-a)} \frac{f(a)}{(x-a)^\alpha} + \sum_{k=0}^{\infty} \frac{f^{(k+1)}(a)}{\Gamma(k+2-a)} (x-a)^{k+1-\alpha}, \tag{0.1} $$

   that is clearly divergent at $x = a$ if $f(a) \neq 0$. This problem is removed by regularizing the fractional derivative, usually by rewriting it in the so-called Caputo form [see, for instance, the paper D. Del Castillo-Negrete, Phys. Plasmas **13**, 082308 (2006) for details.].

7. **Page 8. The paragraph above the Eq. (27). We wonder why the power-law decay is only observed for one of the two tails and the other tail decays exponentially fast? We also want to know why the exponential tail is found in the limit $y \to 0^\pm$ for $\lambda \to \mp 1$. Could you give us some detailed explanations or references we can**

   This behaviour of the extremal Lévy distributions is characteristic and well documented. Mathematically, the reason is that the constants in front of the power-law scalings for large value of their arguments are proportional to $(1 \pm \lambda)$. Thus, one of them does vanish when $|\lambda| = 1$, which is what defines the extremal, Levy distribution. There is an excellent introduction to these pdfs in the first chapter of the wonderful book by Samorodnitsky and Taqqu, "*Stable non-Gaussian random processes*", Chapman & Hall, New York (1994).

8. **Around this paper, we can see the authors give us the numerical simulations and confirm the constant α and β according to the simulations. And we want to know how close this sandpile model simulates the natural moving of the sandpile. Could you give us some specific examples?**

   Again, it was never our intention to claim that this cellular automata is a good model for any realistic, natural sandpile. We only use as a proxy to test basic dynamic features of systems in which self-organized criticality may be relevant. Natural sandpiles are however not well described by SOC models, as shown by many authors (see, for instance S. Nagel, Rev. Mod. Phys. **64**, 321 (1992) or J. Feder, Fractals **3**, 431 (1995)).

List of changes.-

1. Changes have been made to the title, the abstract and the main text to remark that the current study is focused on the running sandpile automaton, with no relation to real running sandpiles. To that effect, we have explicitly used the term "running sandpile automaton" or "running sandpile cellular automaton" generously, instead of just "running sandpile". We have also explicitly stated that real sandpiles are not well modelled by this type of cellular automata, and provided two new references in that regard [Nagel's (Ref. 9) and Feder's (Ref. 10)].

2. The introduction to the sandpile has been extended at the beginning of Sec. 2, as requested by the referee. In particular, we have added explanations for the two conditions pointed out by the referee (i.e., $N_f > P_0 N_b L$ and $Z \simeq -(Z_c - N_f/2)$).

3. We have replaced the use of "limit" by "asymptotic behaviour" where appropriate throughout the text, as advised by the referee.

4. We have reworded the last paragraph before Sec. 4 to make our points clearer to understand.

5. We have added an explanation about the divergence at the start/end point of truncated RL fractional derivatives to Appendix B. We have also pointed the reader to that Appendix when this fact is mentioned in page 8.

6. Minor typos and some small grammatical errors have been amended throughout the text.

Reply to the referee second review on the manuscript: "Modelling transport across the running sandpile by means of fractional transport equations", by R. Sanchez et al

We would like to thank again the referee for his/her interest in our paper and for the time he/she might have devoted to reading it. In what follows, we provide separate and detailed answers to the referee's second set of comments (marked in bold+italics). We have tried to comply with all the requests made by the referee as much as possible, as reflected in the following paragraphs.

Replies to the referee's comments.-

The authors have improved the paper according to the previous comments. We are grateful for the efforts. However we still think some detail points of paper are not accurate and some recisions are needed.

1. **The expression '$Z \simeq -(Z_c - N_f/2)$' still needs further clarified. So far as we know, when the toppling happens in the i-th cell for instance, the system will move N_F grains from i-th cell into the $(i+1)$-th cell. Thus the slope between these 2 cells is $-(Z_c - 2N_f)$ and the average slope of the whole cells is $-(Z_c - N_f)$ instead of $-(Z_c - N_f/2)$. Moreover, the authors say the simulations proves the expression, however we can?t find the simulation results in the first revision paper. Could you please add the simulation results into the paper?. Please make detailed descriptions.**

   After reviewing our previous response to the referee regarding why $Z \simeq -(Z_c - N_f/2)$, we acknowledge that the explanation was not correct. We apologize for having been careless. We provide the correct explanation in what follows. However, we would like to state first that $Z \simeq -(Z_c - N_f/2)$ is an old result for the running sandpile, going at least as back as the late 90s, which is why we did not include any explanation in our submission.

   A direct calculation of the average slope of the running sandpile was made, under certain assumptions, in Mevdevev & Diamond, PRE 58, 6824 (1998). Their result corresponds to their Eq. (11) that contains, in addition to Z_c and N_f various toppling probabilities. In the slowly-forced, non-overdriven, SOC regime, it follows that both p_0 and α in Eq. 11 are small so that, for $1 << N_F << Z_c$, the average slope reduces to $-(Z_c - N_F/2)$. Their calculation is however complicated and difficult to extend beyond the *zero*-dimensional case (i.e., a single cell), although they describe a way to do it numerically.

   We provided recently an alternate argument in Mier & al, PRE 94, 022128 (2016) in the context of the slowly-driven, non-overdriven one-dimensional sandpile. The argument was illustrated in Fig.2 of that paper (see Fig. 1 of this response). Since $h(L) = 0$, the upper limit on the height of the $L-1$ cell is $h_u(L-1) = Z_c$ since, otherwise, avalanches will quickly ensue. At the same time, the lower limit of the height at cell $L-1$ is $Z_c - N_F$. Therefore, its mean height value is $h_a(L-1) = [h_u(L-1) + h_l(L-1)]/2) = Z_c - N_F/2$. Since $h(L) = 0$ (anything that falls on the last cell is instantaneously removed!), $-(Z_c - N_F/2)$ is the average slope at cell $L-1$. The same argument

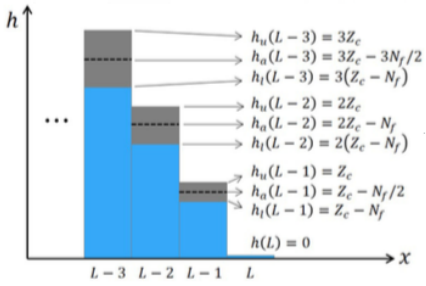

FIG. 2. Scheme with the possible values of h for the last four cells of the sandpile (case $D_0/P_0 = 0$). h_u,h_a, and h_l stand for the upper, average, and lower values of the height, respectively. $h(L) = 0$ is the boundary condition for the bottom cell. Since $h(L) = 0$, the upper limit on the height of the previous cell is $h_u(L-1) = Z_c$. Hence, $h(L-1) \leqslant h_u(L-1)$. But $h(L-1) \geqslant h_l(L-1) = Z_c - N_f$ to satisfy the steady state condition. Thus, its mean value is $h_a(L-1) = [h_u(L-1) + h_l(L-1)]/2 = Z_c - N_f/2$. The same principle can then be applied inwards.

Figure 1: Fig. 2 of Mier & al, PRE 94, 022128 (2016).

can be applied inwards. Starting at cell $L-2$, the maximum height there will be $h_u(L-2) = 2Z_c$, since Z_c is the maximum stable increment with respect to the maximum height of cell $L-1$, that is given by $h_u(L-1) = Z_c$. The minimum height for cell $L-2$ will be $h_l(L-2) = 2Z_c - 2N_F$, since it will be reached after removing N_F from the $(L-2)$ cell when its relative height with respect the last cell is Z_c, but with the latter being at its minimum height, $h_l(L-1) = Z_c - N_F$. Thus, the average height of the $L-2$ cell is $h_a(L-2) = (h_u(L-2) + h_l(L-2))/2 = 2Z_c - N_f$. And the mean gradient between the $L-2$ and $L-1$ cell is $Z_a(L-2) = h_a(L-2) - h_a(L-1) = Z_c - N_F/2$. The same argument can be propagated all the way to the sandpile center!

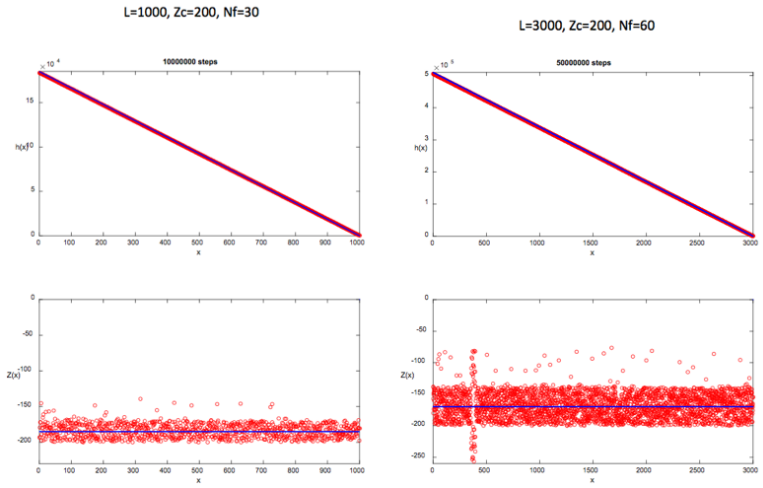

Figure 2: Instantaneous height and slope for two running sandpile cases. The average slope (shown in blue) is -184.26 for the left case, and -170.43 for the right one. The value of the estimate $-(Z_c - N_F/2)$ is, respectively, -185 and -170.

.

The soundness of this argument can also be proved numerically. For instance, in Fig. 2 we show the plot of the instantaneous height and slope profiles at steady state for two different sandpiles, one with $L = 1000$, $N_F = 30$ and $Z_c = 200$ (left) and another with $L = 3000$, $Z_c = 200$ and $N_F = 60$. In them, some avalanching events are also apparent! The average slope is shown in blue,

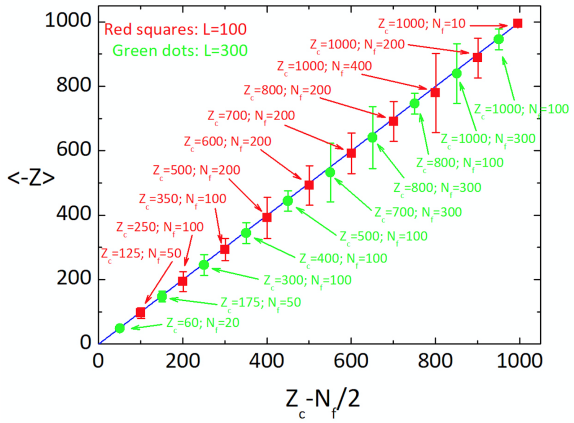

Figure 3: Plot of the average slope $-\langle Z\rangle$ vs $Z_c - N_F/2$ for two sandpile runs (one with size $L = 100$, another with $L = 300$) with different values Z_c and N_F.

having a value that correlates very well with $-(Z_c - N_F/2)$. We have also collected the average (over all positions) slopes (i.e., $-\langle Z(x)\rangle$, for two different sandpiles (one with $L = 100$, another with $L = 300$) and varying values of N_F and Z_C and plotted them against $Z_c - N_F/2$ in Fig. 3. As can be seen, the given estimates works pretty well. We have also included error bars that measure the standard deviation of the slope that, as expected, scales with the value of N_F.

Being as it is a pretty old result, we think that it is not appropriate to include a long explanation about this estimate (or a figure) in the submitted paper, even more when considering that the argument has already been published recently in another paper of ours and that the current manuscript is in fact focused on something completely unrelated. However, we have added a brief sentence after this result is stated in the introduction of the sandpile model in which these two references (Mevdevev's PRE of 1998 and our own PRE of 2016) are clearly identified, and where the interested reader can find a justification for this value. We have also added Fig. 3 to the paper, as requested by the referee. We hope that the referee is now convinced by our response, and also that he/she finds this course of action adequate.

2. **Page 3. We still think there is mistake in the derivation of Eq. (14) simply from Eq. (2). The 2 papers which the authors provide simply talk about the random walk on the lattice and utilizing the continuous time random walk model to obtain the equation about PDF. However in this paper, in order to obtain the Eq. (14) by utilizing Eq. (2) and Eq. (3), the propagator must have the form $G(x,t|x',t') = G(x-x',t-t'|0,0)$. Then we can use the property of Fourier-Laplace transform. However, the expression $G(x,t|x',t') = G(x-x',t-t'|0,0)$ indicates the process must be Markovian which the process with power-law waiting time distribution, this paper discussed, does not have.**

We disagree with the referee on this one, since we are certain that our derivation is correct. We will try to justify it in what follows. As it is well-known, a Markovian process is one in which one can advance the state without needing any information about the previous history. If the quantity of interest was the particle density, $n(x,t)$, one would then have that for a Markovian process it is satisfied that:

$$n(x,t) = \int dx' G(x,t|x',t') n(x',t'), \quad \forall t,\ t' \leq t. \tag{0.1}$$

The propagator $G(x,t|x',t')$ gives the probability of a particle that is at x' at time t' being found at x and a later time t. Thanks to this equation being valid for any $t' < t$ for a Markovian process,

one finds by recurring this expression that:

$$n(x,t) = \int dx' G(x,t|x',t') \int dx'' G(x',t'|x'',t'') n(x'',t''), \quad \forall t,\ t' \leq t, t'' \leq t', \tag{0.2}$$

from which it follows that the propagator of a Markovian process satisfies:

$$G(x,t|x',t') = \int dx'' G(x,t|x'',t'') G(x'',t''|x',t'), \quad t \leq t'' \leq t' \tag{0.3}$$

that is the continuous version of the well-known recursive property of the propagator of a discrete Markov chain. If, in addition to being Markovian, the process is also translationally invariant in space and time (that is, if the properties of the process do not depend on the location or time) then one has that,

$$G(x,t|x',t') \to G(x-x',t-t'), \tag{0.4}$$

depending only on the relative distance and the elapsed time.

If the process is **not Markovian**, Eq. 0.1 is no longer appropriate, since the role of the previous history of the system for any time prior to t' cannot be neglected. However, one can still write:

$$n(x,t) = \int dx' G(x-x'|t) n(x',0), \quad \forall t > 0, \tag{0.5}$$

assuming that the process starts at $t = 0$ and that $n(x,0)$ is, in this case, the initial condition for the density. The only condition for Eq. 0.5 to be valid is that the process must be homogeneous (or translationally-invariant) in space, so that the propagator only depends on the relative distance, not explicitly on x'. In contrast to the Markovian case, it is now impossible to find $n(x,t)$ from just the knowledge of the value of the density at a previous time $n(x,t')$, with $t' < t$, since this would imply that the previous history of the process could be neglected. The only exception to this is naturally at $t = 0$, where the process starts. Or, in other words, because $n(x,t) = 0, \forall t < 0$. This is what Eq. 0.5 expresses. The non-Markovian character of the dynamics will be hidden within the specific form of $G(x-x'|t)$ that, as a result, will no longer satisfy the recursive Eq. 0.3.

In our manuscript, Eq. (2) is used to express the general solution of the (non-Markovian) CTRW, that we repeat here for convenience:

$$n(x,t) = \int dx' \int dt' G(x-x'|t-t') S_{\text{aug}}(x',t'). \tag{0.6}$$

We will argue that this formula is perfectly OK for a non-Markovian process since it is completely analogous to Eq. 0.5. The fact that a convolution in time appears may look weird at first. However, it only appears because of our introduction of an augmented source that is given by $S_{\text{aug}}(x,t) = S(x,t) + \delta(t) n(x,0)$. That is, it is the sum of the initial condition $n(x,0)$ plus the source of NEW particles (if any) that is added at each time t. This can be made clearer by considering first that the NEW particles are added ONLY at a collection of discrete times, $\{T_i, i = 1, \cdots N\}$, according to a prescribed profile $S_i(x)$. In that case the equation would become:

$$n(x,t) = \int dx' G(x-x'|t) n(x',0) + \sum_{i=1}^{N} \int dx' G(x-x'|t-T_i) S_i(x), \tag{0.7}$$

which is completely analogous to Eq. 0.5 and perfectly OK to describe an externally-driven (at discrete times), non-Markovian process. The only additional condition is that the process must also be homogeneous in time, so that we can use the same propagator for the sources that are added at each T_i.

If the source is instead continuous in time the sum is replaced by an integral over time and, by introducing the augmented source, the convolution in time appears. Again, the validity of this approach requires only that the process be homogeneous in space and time (or, more precisely, translationally invariant!).

After the validity of Eq. 0.6 has been established, it is then perfectly justified to take its Fourier-Laplace transform to convert it into:

$$n(k,s) = G(k,s)S_{\rm aug}(k,s), \tag{0.8}$$

and then use the propagator of the translationally-invariant CTRW (calculated originally in Montroll & Weiss, J. Math. Physics 6, 167 (1965).) in order to derive our effective fractional transport model. Indeed, the symmetry requirements previously mentioned are fully satisfied, since the pdfs $p(\Delta x)$ and $\psi(\Delta t)$ that define the CTRW do not depend explicitly on the current position or time.

In order to make these ideas clearer in the manuscript, we have added a few sentences explaining all these points just after Eq. (2) in page 3. We hope that it helps to explain better how this is done and how the validity of Eq. (2) is not limited to Markovian processes.

3. **We are still confused about the divergent of $n(x,t)$ at the starting point x = 0. From the authors explanation, we don't think the divergent of fractional derivative of a regular function at starting point $x = 0$ indicates the solution of fractional derivative equation diverging. Please check.**

It might be that we have not explained ourselves adequately. What we meant in our manuscript is that, although the unbounded fractional differential equation expressed in terms of Riemann-Liouville (R-L) fractional derivatives has smooth solutions, the truncation of the R-L fractional operators to a finite domain may introduce divergences at the starting/ending points of the boundary **when one prescribes specific initial and boundary values for the solution in terms of its integer derivatives, as it is the usual situation in physical problems**. As discussed by Podlubny (see I. Podluby's *Fractional Differential Equations*, page 78-79), this could be avoided by prescribing instead all boundary and initial conditions in terms of R-L fractional derivatives, but this choice is difficult to justify physically. It is for this reason that many authors avoid these divergences when specifying boundary/initial values by replacing the R-L fractional derivative by a fractional derivative of the Caputo type, that does not have this problem. D. Del Castillo-Negrete illustrates this fact very well (see D. Del Castillo-Negrete, Phys. Plasmas **13**, 082308 (2006)).

The mathematical reason for the divergence is the one we gave in our previous answer. Let's take, for instance, the left-sided Riemann-Liouville fractional derivative of order $0 < \alpha < 1$ (this is the derivative that appears in the asymmetric Riesz-Feller derivative of order α in our Eq. 16) of a regular function $f(x)$, it is found to be:

$${}_aD_t^\alpha f(x) = \frac{1}{\Gamma(1-a)}\frac{f(a)}{(x-a)^\alpha} + \sum_{k=0}^{\infty}\frac{f^{(k+1)}(a)}{\Gamma(k+2-a)}(x-a)^{k+1-\alpha}, \tag{0.9}$$

by considering the Taylor expansion of $f(x)$. Here, one just need to use that the fractional derivative of a power law is given by (see Podluby's *Fractional Differential Equations*, page 72-73),

$${}_aD_t^\alpha (x-a)^k = \frac{\Gamma(k+1)}{\Gamma(k+1-\alpha)}(x-a)^{k-\alpha}. \tag{0.10}$$

Clearly, the first term in Eq.0.9 is divergent at $x = a$ if one chooses a boundary condition such as $f(a) \neq 0$. It would be regular, however, if one chooses as boundary condition ${}_aD_t^\alpha f(a) = 0$, but it is difficult to find a physical interpretation of what such condition means in most cases.

We have modified the wording in the paper a bit at the end of Sec. V and in Appendix B to try to make this point come across more clearly.

List of changes.-

1. We have added a brief clarification in parenthesis after $< Z > \simeq -(Z_c - N_F/2)$ first appears in the introduction of the sandpile model that directs the interested reader to two references (Mevdevev's PRE of 1998 and our own PRE of 2016) in which this value is provided. We have also added a new figure (Fig. 3) to the paper, that proves the validity of this statement numerically, as requested by the referee.

2. We have added a few sentences explaining why our approach is adequate for Non-Markovian processes just after Eq. (2) in page 3.

3. We have reworded a bit the last paragraph of Sec. V and Appendix B to try to explain more clearly the issue with the regularization of R-L fractional derivatives raised by the referee.

Replies to the original referee's third review and to the second referee's comments on the manuscript: "Modelling transport across the running sandpile by means of fractional transport equations", by R. Sanchez et al

We would like to thank again the referees for their interest in our paper and for the time they might have devoted to reading it. In what follows, we provide separate and detailed answers to the referee's third set of comments (marked in bold+italics) and the comments made by the new referee. We have tried to comply with all the requests made by the referees as much as possible, as reflected in the following paragraphs.

Replies to the first referee's third set of comments.-

The paper is making some fundamental mistakes. It seems that the authors do not really understand what is Markov process. The propagator of the CTRW model with first moment diverging power-law waiting time is None Markov; may you refer to Metzler and Klafter's Physical Report paper published in 2000. Mathematically, it can also be proved that the governing equation for the propagator does not have semigroup properties.

Response: We think that the referee is the one who does not really understand our paper. It might be that we have not been able to explain ourselves correctly, but we have never meant to say that the CTRW model **with first moment diverging power-law waiting times** is a Markov process. In fact, we agree completely with the referee that it is NOT a Markov process. That is precisely the reason why we start our derivation from Eq. 2, that is valid for non-Markovian processes as we extensively showed in our previous response to the referee. We do not know what more to say about this. We are however relieved that the (new) second referee agrees with us on this.

Replies to the second referee's new set of comments.-

This paper deals with the statistical analysis of the sandpile cellular automaton originally proposed by Hwa and Kardar. In particular the authors pursue a CTRW style analysis based on a fully asymmetric Levy stable jump length distribution. The manuscript has gone through two rounds of refereeing, and the authors modified their paper accordingly. In his third report the referee states that the CTRW process with non-Poisson waiting time density is not Markovian and thus the derivation of the final propagator in Laplace-Fourier space were not correct.

Indeed, the CTRW process in general is not Markovian. However, locally it is Markovian, as waiting times are annealed, i.e., identically distributed and independent random

variables. Only the accumulation of waiting times, which do not possess a first moment, introduce a memory and thus non-Markov properties. This is indeed reflected in the s^β dependence of the final solution in Laplace-Fourier space. This maybe somewhat bizarre property was called semi-Markov property by Scher and Montroll, see also the beautiful book by Barry Hughes on random walks & random environments. As far as I can see the derivation is sound, and the transformations applicable. I thus recommend to accept the manuscript after the authors include the following changes:

(1) The authors should clarify the semi-Markov property in a short paragraph. They should mention that, apart from the very choice of the jump length distribution, this is standard CTRW and/or fractional dynamic equations.

(2) The authors should distinguish the inclusion of an external drift by an asymmetry in the left-right jump likelihoods (while keeping the jump length distribution symmetric), as discussed in Ref [28], and from a different point of view in PRE 59, 2736 (1999). I am also sure that there are papers discussing asymmetric Levy stable jump length densities in literature, for instance, Mark Meerschaert worked on this. I am travelling & cannot check in detail, so I ask the authors to make sure that they perform some literature research here.

RESPONSE: We agree with the second referee completely. We are very satisfied that he/she understands our approach and also that he/she finds it adequate. We have added a couple of sentences to the manuscript (at the beginning of Sec. III, just before Eq. 2) describing the semi-Markov property and also mentioning that the method we follow is standard in the field. We have also introduced a sentence pointing out the difference in CTRW between the consideration of an asymmetry in the jump distribution and the introduction of a drift, and added some references as advised (also in Sec. III, a few sentences before Eq. 12).

List of changes.-

1. We have added a sentence at the beginning of Sec. III, just before Eq. 2 mentioning the semi-Markov property of the CTRW with waiting-times with a divergent first moment.

2. We have added a sentence in Sec. III, just before Eq.12 making the distinction between a fully-asymmetric step-size pdf and the introduction of a drift.

3. The labels of some figures have been modified as requested by the editors to replace "cells" by "in cells", "steps" by "in steps" and so forth.